


Seismic vulnerability assessment using association rule learning: application to the city of Constantine, Algeria

Abdelheq Guettiche^{1,2}  · Philippe Guéguen³ ·
Mostefa Mimoun²

Received: 27 May 2016 / Accepted: 27 December 2016 / Published online: 2 January 2017
© Springer Science+Business Media Dordrecht 2017

Abstract We performed a seismic vulnerability assessment of the city of Constantine (Algeria) using the Risk-UE and datamining-based methods [association rule learning (ARL)]. The ARL method consists in establishing relationships between building attributes (number of stories or building age) and the vulnerability classes of the European Macro-seismic Scale, EMS98. This approach avoids the costly process of drawing up an inventory of building characteristics in the field, which often discourages the assessment of seismic risk initiatives in weak to moderate seismic-prone regions. We showed that the accuracy of the assessment is independent of the subset used for the learning phase leading to development of the Constantine vulnerability proxy. Considering only two attributes, the vulnerability assignment is equal to about 75%, reaching 99% if material is added to the attributes considered. Comparison of Risk-UE and ARL results revealed a reliable assessment of vulnerability, the differences having only a slight impact on the probability of exceeding the damage level computed by EMS98 or Risk-UE in Constantine. The results of this study suggest that the ARL-based vulnerability proxy is efficient and could be applied to the rest of Algeria.

Keywords Vulnerability · Scenario · Earthquake · Association rule learning · Risk-UE · Damage grade · EMS98 · Constantine

✉ Philippe Guéguen
Philippe.gueguen@univ-grenoble-alpes.fr

¹ Centre Universitaire Abdelhafid Boussouf, Mila, Algeria

² Civil Engineering Department, Université des Frères Mentouri, Constantine, Algeria

³ Institut des Sciences de la Terre – ISTerre, Université de Grenoble Alpes/CNRS/IFSTTAR, Grenoble, France

1 Introduction

In order to reduce risk, several seismic-prone cities around the world (Tucker et al. 2013), such as Quito in Ecuador (Chatelain et al. 1999), Kathmandu in Nepal (KVERMP 1998), Istanbul in Turkey (Erdik et al. 2003), Catania in Italy (Faccioli et al. 1999) and Nice in France (Bard et al. 2005), have been analyzed in terms of seismic risk, with the objectives of educating the public, producing seismic scenarios to simulate losses and operational problems and implementing an action plan to manage seismic risk. Benson and Twigg (2004) claim that with \$40 million invested in preventive measures worldwide in the 1990s, economic losses have been reduced by \$280 million. They also support the view of emergency specialists, who are increasingly insistent on the need to invest in preparation, prevention and disaster attenuation measures, such as those supported by seismic scenarios, to reduce losses. Moreover, seismic risk scenarios are useful to study the best investment framework for the seismic retrofitting of buildings that can be attractive against the effects of long return periods events (Smyth et al. 2004). In fact, predicted damage in existing structures is the key parameter to anticipate direct and indirect seismic losses and fatalities. Consequently, before simulating and testing losses, efforts must be concentrated on the seismic vulnerability assessment of existing structures at urban or regional scales, such as in Algeria, a region whose first seismic code dates back to 1981 for public buildings. Assuming a small rate of renewal, the majority of constructions of Algeria's building stock were therefore built with no seismic design engineering and can be considered vulnerable to regional earthquakes, as demonstrated by the 2003 Boumerdes earthquake where many reinforced concrete buildings were extensively damaged (Meslem et al. 2012).

Assessing vulnerability at the urban scale is a complex task due to the number of buildings concerned, their heterogeneities in terms of structural design and seismic response and the lack of main information concerning their design (Guéguen 2013). Macro-scale methods have been developed, based on data collected in the field during post-seismic periods. They propose damage functions calibrated on observed damage and building typology, as proposed by the Federal Emergency Management Agency (FEMA) in the USA (Hazus 1997), the Gruppo Nazionale per Difesa dai Terremoti in Italy (Benedetti and Petrini 1984; GNDT 1993) or the Risk-UE method developed within the framework of the European project (Spence and Brun 2006; Lestuzzi et al. 2016). Barbat et al. (2010) published a review of the seismic vulnerability assessment methods for urban application. Whatever the method, the difficulty remains to inventory the buildings, involving costly visual screening throughout the city. This is even more complex in moderate seismic-prone regions, where resources for seismic evaluation are often difficult to mobilize and are limited (Guéguen et al. 2007), even though the seismic hazard is not negligible.

Recently, simplified macro-scale methods have been adapted to reduce the inherent cost of the building in situ surveys at the urban scale. Such initiatives consist in simplifying the visual screening stage by considering only the key parameters whose contribution to seismic vulnerability is significant (Guéguen et al. 2007) or by using remote sensing methods (Mueller et al. 2006; Geiß et al. 2014; Riedel et al. 2015). Datamining-based methods have also been developed to derive the best proxy linking the building features, easily assessed by remote sensing or from preexisting databanks (e.g., national census), with the seismic vulnerability of buildings (Riedel et al. 2014, 2015).

In this study, we propose to validate this approach in a seismic-prone city, Constantine in Algeria, for which an extensive vulnerability assessment using the Risk-UE method is available. After presenting the seismic context and urbanization of Constantine, the method is developed and applied to the city. In the last section, the results are compared with those of the Risk-UE method, before concluding on the efficiency of this approach.

2 The city of Constantine

The city of Constantine (Fig. 1 a) is located in the northern part of Algeria. The tectonic context of the Constantine region results from the convergence of the Eurasian and African plates. Descriptions of the tectonic context can be found in the abundant literature (e.g., McKenzie 1972; Aoudia and Meghraoui 1995; Mickus and Jallouli 1999; Yelles-Chaouche et al. 2006; Hamdache et al. 2012). As a result, this region is one of the most seismically active regions of the Mediterranean (Buforn et al. 1995; Kherroubi et al. 2009), characterized by intense seismic activity. This activity mainly affects the northern part of Algeria, home to the most important cities, i.e., the country’s most densely populated cities, concentrating housing, infrastructures, economic and industrial activities.

The city is exposed to a complex and moderate to strong seismic hazard (Peláez et al. 2006; Baba Hamed et al. 2013). The Ain Smara Fault, situated southeast of Constantine

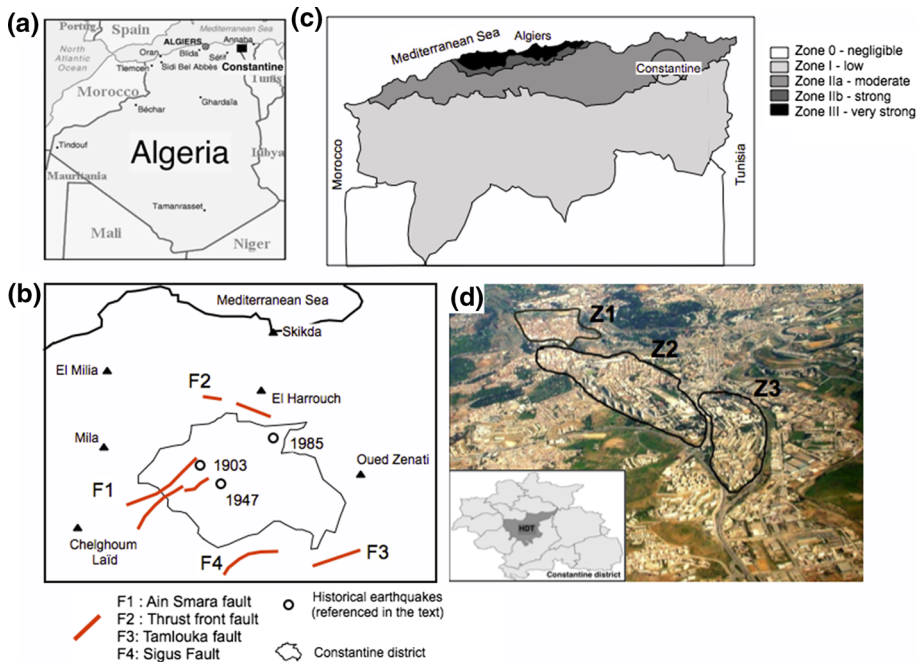


Fig. 1 a General situation of the city of Constantine in Algeria. b Location of the main fault and historical earthquakes mentioned in the text (after Bounif et al. 1987). c Seismic macro-zoning map of Algeria (after RPA03 2003). d Location of the historic downtown area concerned by this study and aerial view of HDT with subzones Z1, Z2 and Z3 described in this study

(Fig. 1b), is a major active fault and a primary source of earthquakes affecting the Eastern Tellian Atlas (northeast Algeria) confirmed by surface ruptures observed after the 1985 earthquake (Bounif et al. 1987). This fault can be considered as an important potential source of seismic activity according to the probabilistic seismic hazard study done for Algeria (Peláez et al. 2006; Fig. 1c). It generated the strongest earthquake in 1908, 1947 and in 1985, the latest corresponding to the strongest event recorded since the implementation of instrumental seismology (Bounif et al. 1987; Ousadou et al. 2013), causing significant damage in Constantine (Ms = 5.9, October 27, 1985), with macro-seismic intensities ranging from IX to X.

Constantine has about 1 million inhabitants according to the last census of National Office of Statistics in 2008 (Office national des statistiques, ONS 2008). It is a very active city in social, economic and industrial terms, considered to be the third most important city in Algeria. It is also famous for its cultural heritage buildings, including constructions of urban and architectural value. Analysis of the Constantine city has been performed in the past using Hazus method (Boukri et al. 2014) with concluding to a high vulnerability of the city. For our study, the inventory phase covered only the historic downtown area (HDT, Fig. 1d), for the collection of building details required for the seismic vulnerability assessment using the Risk-UE method (Milutinovic and Trendafiloski 2003). According to official statistics published by the ONS (2008), this area is characterized by a dense, old stock of residential buildings and is highly populated, with 448,374 inhabitants that correspond to 2089 inhabitants/km².

In total, 2252 buildings were surveyed by visual screening, collecting data on the state of conservation and on all structural and non-structural characteristics. A specific technical form was established (Appendix 1) for building by building inspection, after consultation with the direction in charge of the urban planning and construction in Constantine (Direction de l'Urbanisme et de la Construction Constantine, DUC) and the Technical Control of Construction (CTC) in Constantine, also with the help of several technical reports and documents available on the building construction in Constantine. Moreover, a specific datasheet was developed to compute the vulnerability index and the associated damage (Appendix 1). The building inventory is certainly the most time-consuming step of the seismic vulnerability assessment process. It took 3 years to collect detailed information on the design and construction types of Constantine's buildings according to Risk-UE attributes, i.e., type of material (masonry, reinforced concrete, steel), year of construction classified into six classes, number of floors, in plan and elevation irregularities, state of maintenance, aggregation conditions for distinguishing stand-alone, middle, corner or header building (i.e., adjacent with another building on one side or on two or more sides), and information on soil morphology (cliff or slope). Vulnerability indexes by typology and modifiers used for Risk-UE are given Tables 1 and 2, respectively. At the same time, each building was classified according to the European Macro-seismic Scale typology (EMS98, Grünthal and Levret 2001).

This information was fed into the Constantine Building Databank (CBD). Moreover, the national Algerian organism of technical and building inspection done in 2009 during a detailed but partial field survey confirmed the CBD information, by crossing modifiers and vulnerability assessment for several buildings. Finally, the HDT was divided into three zones (Z1, Z2 and Z3) according to the historic urbanization of the area (Fig. 1d). In Z1, about 63% of the total building stock (1887 buildings) was surveyed (i.e., 1185 buildings), in Z2 about 83% (1016/1221) and about 41% in Z3 (51/123). The distribution of surveyed buildings according to building material reflects the evolution of construction methods and

Table 1 Representative values of vulnerability indexes for each class of the building typology used in Risk-UE (after Milutinovic and Trendafiloski 2003)

Typology	Description	Representatives vulnerability index IV				
		IV ^{min}	IV ⁻	IV*	IV ⁺	IV ^{max}
M1.1	Rubble stone	0.62	0.81	0.873	0.98	1.02
M1.2	Simple stone	0.46	0.65	0.74	0.83	1.02
M1.3	Massive stone—Ashlar	0.3	0.49	0.616	0.793	0.86
M2	Adobe (earth bricks)	0.62	0.687	0.84	0.98	1.02
M3.1	Wooden slabs—Hardwood	0.46	0.65	0.74	0.83	1.02
M3.2	Masonry arches	0.46	0.65	0.776	0.953	1.02
M3.3	Composite steel and masonry slabs	0.46	0.527	0.704	0.83	1.02
M3.4	Reinforced concrete slabs	0.3	0.49	0.616	0.793	0.86
M4	Reinf. masonry load-bearing walls	0.14	0.33	0.451	0.633	0.7
M5	Structures made completely of reinforced masonry	0.3	0.49	0.694	0.953	1.02
RC1	Concrete moment frame	-0.02	0.047	0.442	0.8	1.02
RC2	Concrete shear walls	-0.02	0.047	0.386	0.67	0.86
RC3.1	Regular infilled walls	-0.02	0.007	0.402	0.76	0.98
RC3.2	Irregular frames	0.06	0.127	0.522	0.88	1.02
RC4	RC dual system (frame and walls)	-0.02	0.047	0.386	0.67	0.86
RC5	Precast concrete tilt-up walls	0.14	0.207	0.384	0.51	0.7
RC6	Precast RC frames and shear walls	0.3	0.367	0.544	0.67	0.86
S1	Steel moment frames	-0.02	0.467	0.363	0.64	0.86
S2	Steel braced frames	-0.02	0.467	0.287	0.48	0.7
S3	Steel frames + unreinf. mas. infill w	0.14	0.33	0.484	0.64	0.86
S4	Steel support beams/columns with structural concrete wall cast in situ	-0.02	0.047	0.224	0.35	0.54
S5	Steel and reinforced concrete components	-0.02	0.257	0.402	0.72	1.02
W	Wood structure	0.14	0.207	0.447	0.64	0.86

urbanization trends: Unreinforced masonry buildings represent 94% of the whole buildings in Z1, 64% in Z2 and 0% in Z3.

A general description of the CBD is shown in Fig. 2. In this figure, buildings are grouped according to four attributes: (1) period of construction, according to the historic urbanization of the city and evolutions in Algerian design code; (2) number of stories, defined according to the interval given in the Risk-UE method, i.e., low-rise (1–2), mid-rise (3–5) and high-rise (>6) buildings; (3) type of material found in the studied area, i.e., reinforced concrete (RC), unreinforced masonry and steel; and (4) roof shape (slope or flat). These four attributes were selected for their ease of observation, with no attribution error, on the urban scale. In total, 78% of the buildings surveyed were unreinforced masonry, 21% reinforced concrete and only 1% steel. The CBD contains 2252 buildings:

- 448 built before 1837, composed mainly of unreinforced masonry buildings in adobe and rubble stone,
- 744 from 1837 to 1920, corresponding to unreinforced masonry and RC buildings;
- 819 between 1921 and 1962, corresponding to the generalization of reinforced concrete in buildings but without application of any seismic code measures;

Table 2 Scores for the vulnerability modifiers used for masonry and reinforced concreted buildings, adapted from Risk-UE (after Milutinovic and Trendafiloski 2003) to the Constantine city

Vulnerability factors	Masonry		Reinforced concrete			
	Parameters	IV_M	Parameters	Low code	IV_M Medium code	High code
Code level	N/A			+0.16	0	-0.16
State of preservation	Good	-0.04	Good		N/A	
	Bad	+0.04	Bad	+0.04	+0.02	0
Number of floors	Low (1 or 2)	-0.02	Low (1 or 2)	-0.04	-0.04	-0.04
	Medium (3, 4 or 5)	+0.02	Medium (3–5)	0	0	0
	High (6 or more)	+0.06	High(6 or more)	+0.08	+0.06	0.04
Soft story	Demolition/ transparency	+0.04		N/A		
Plan irregularity		+0.04	Shape	+0.04	+0.02	0
			Torsion	+0.02	+0.01	0
Vertical irregularity		+0.02		+0.04	+0.02	0
			Short columns	+0.02	+0.01	0
			Bow windows	+0.04	+0.02	0
Retrofitting interventions		-0.08 +0.08	Bad mainten.	+0.04	+0.02	0
Aseismic devices	Barbican, foil arches, buttresses	-0.04	N/A			
Aggregate effect: position	Middle	-0.04	Insufficient joint	+0.04	0	0
	Corner	+0.04				
	Header	+0.06				
Aggregate building: elevation	Staggered floors	+0.02	N/A			
	Buildings of different heights	-0.04 +0.04				
Foundations	Foundations at different levels	+0.04	Beams	-0.04	0	0
			Connect. beams	0	0	0
			Isolated footing	+0.04	0	0
Soil morphology	Slope	+0.02	Slope	+0.02	+0.02	+0.02
	Cliff	+0.04	Cliff	+0.04	+0.04	+0.04

- 119 from 1963 to 1981;
- 38 between 1982 and 2003;
- 84 after 2003.

Most of the constructions of the last three periods are RC buildings. The two first periods correspond to the Ottoman and French epochs, representing approximately 50% of buildings surveyed herein. Almost all buildings (94%) were erected before publication of the first Algerian seismic code in 1981 (RPA81 1981), therefore considered as non-engineered buildings, 2% were designed between 1981 and publication of the latest version of

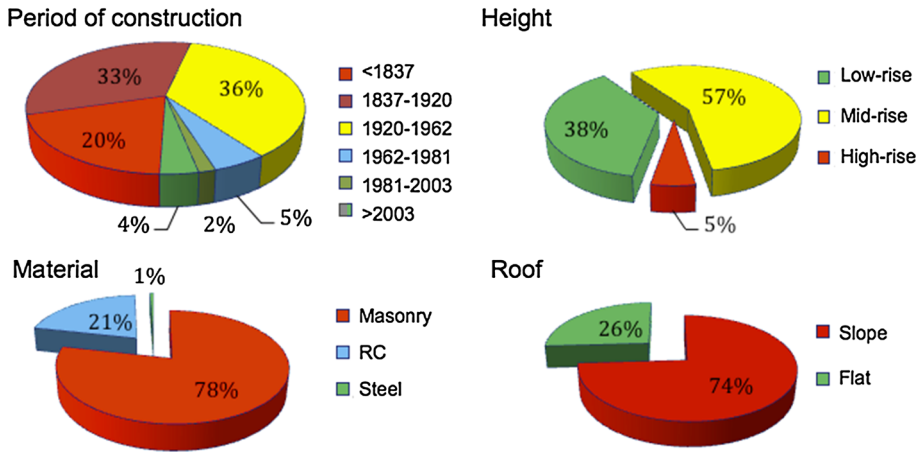


Fig. 2 Description of the number of buildings surveyed in this study according to four attributes: period of construction, number of floors, material type and roof shape

the Algerian seismic code of 2003 (RPA03 2003), considered as buildings with moderate seismic design according to Risk-UE (moderate code), and only 4% of construction were built after 2003, considered as high seismic design (high-code) buildings. Moreover, the study contains about 120 high-rise buildings, which represent only 5% of the building stock, 845 (38%) and 1287 (57%) buildings being classified as low-rise and mid-rise, respectively.

Table 3 Distribution of surveyed buildings by Risk-UE typology

Typologies EMS98	Building types Risk-UE	Nb	%	Total %
Unreinforced masonry	M1.1: rubble stone	105	4.66	78.60
	M1.2: simple stone	304	13.50	
	M1.3: massive stone—Ashlar	903	40.10	
	M2: adobe (earth bricks)	446	19.80	
	M3.1: wooden slabs—Hardwood flooring	2	0.09	
	M3.4: reinforced concrete slabs	9	0.40	
Reinforced masonry	M4: reinf. masonry load-bearing walls	1	0.04	20.78
Reinforced concrete	RC1: concrete moment frame	281	12.48	
	RC2: concrete shear walls	76	3.37	
	RC3.1: regular infilled walls	80	3.55	
	RC3.2: irregular frames	1	0.04	
	RC4: RC dual system (frame and walls)	6	0.27	
	RC5: precast concrete tilt-up walls	22	0.98	
	RC6: precast C frames and shear walls	2	0.09	
Steel	S.1: steel moment frames	2	0.09	0.62
	S.2: steel braced frames	8	0.36	
	S.3: steel frames + unreinf. mas. infill w	4	0.18	
Total		2252	100	100

Table 3 shows the distribution of buildings classified according to the Risk-UE typology (Milutinovic and Trendafiloski 2003). Solid stone, class M1.3 (called Ashlar), and adobe, class M2, are the most representative typologies in the building stock surveyed. Compared with the EMS98 typology, the vulnerability classes range from A (most vulnerable) to F (least vulnerable), with 99% of unreinforced masonry buildings in classes A and B, 75% of RC buildings in class C and the remaining 25% being divided among classes D and E. The vulnerability reflects the low seismic design of the existing RC and unreinforced masonry buildings, built before the issue of the first Algerian seismic code.

3 Methods

The flowchart of the methods followed in this study is shown Fig. 3, each branch being explained in this section.

3.1 Brief description of Risk-UE level 1

In the first step, the seismic vulnerability assessment of zones 1–3 was computed using the Risk-UE method, considered as the reference assessment method in this study. Risk-UE

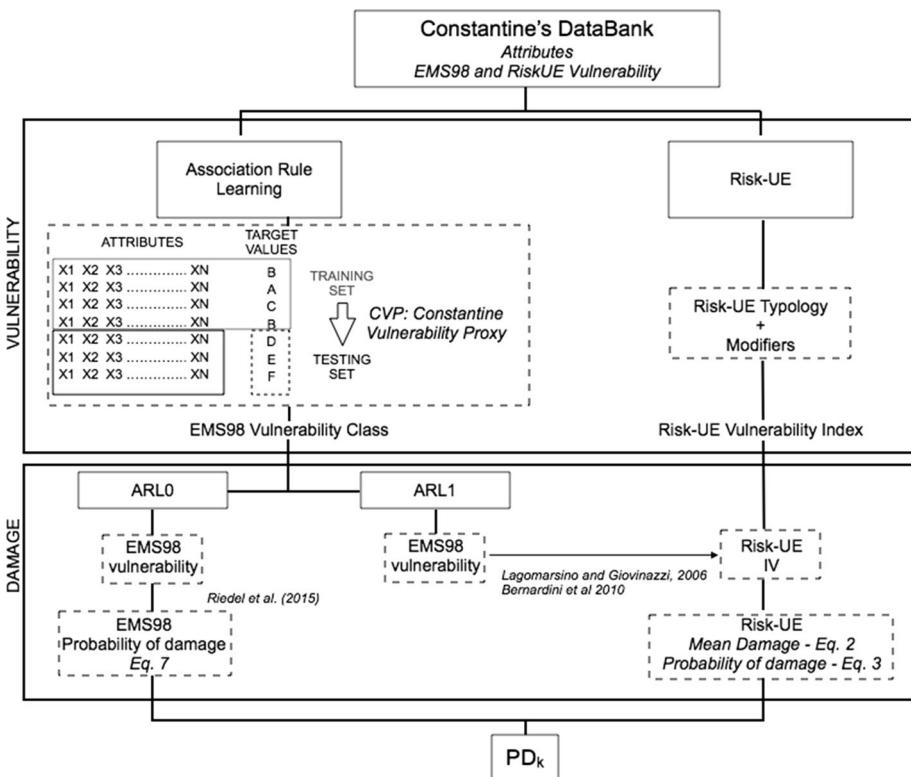


Fig. 3 Flowchart of the methods followed in this study

vulnerability assessment method was developed for the eponymous European project considering seven major European cities (Spence and Brun 2006). At first time, the method consists classifying each building into the typology defined by the materials and/or structural systems. Basic vulnerability indexes are attributed to each typology class (Milutinovic and Trendafiloski 2003) corresponding to the median value IV^* and to the lower IV^- and upper IV^+ bounds of the possible values of the vulnerability index. Modifier factors are then applied to IV^* , to take into account height, irregularities, position, etc. The final vulnerability index, independent of the hazard, is the sum of IV^* and the weighted values of the modifier factors as follows:

$$IV = IV^* + \Delta V_M + \Delta V_R \tag{1}$$

where ΔV_M represents the seismic behavior modifiers and ΔV_R is a regional vulnerability factor (considered equal to 0). Once vulnerability has been assessed, the average damage grade μ_D is given by the following equation:

$$\mu_D = 2.5 \left[1 + \tanh \left(\frac{I + 6.25IV - 13.1}{2.3} \right) \right] \tag{2}$$

where I is the seismic hazard described in terms of EMS98 macro-seismic intensity. μ_D varies from 0 (no damage) to 5 (severe damage or destruction) following the six-level damage scale D_k given in EMS98, with six grades (k [0, 5]) ranging from no damage (D0) to complete destruction (D5). The binomial distribution proposed in Lagomarsino and Giovinazzi (2006) and adjusted to post-earthquake observation is then used to give damage as the probability $P(D_k)$ of reaching each damage grade D_k (k [0, 5]) for a given μ_D as follows:

$$P(D_k) = \frac{5!}{k!(5-k)!} \left(\frac{\mu_D}{5} \right)^k \left(1 - \frac{\mu_D}{5} \right)^{5-k} \quad (!: \text{factorial operator}). \tag{3}$$

The vulnerability curves are then plotted after computing the probability density function $P(D_k)$ for each vulnerability class. For each class of vulnerability and each intensity, they represent the probability of exceeding a degree of damage k for a given intensity (Fig. 4).

3.2 Association rule learning classification

The building-by-building inventory of structural attributes is certainly the most costly step in any process to estimate seismic vulnerability at an urban scale. Riedel et al. (2014) thus propose a datamining-based method for developing a seismic vulnerability proxy using basic attributes. There is no doubt that additional information such as material or resistance of structural elements contributes to the vulnerability of existing buildings. However, datamining consists in discovering patterns and trends that go beyond simple analysis, and finding “hidden” correlations among different attributes and targets in large databanks. In the field of seismic vulnerability assessment, it consists in establishing correlations using mathematical algorithms (if/then statements) between basic attributes that are easily available (e.g., number of stories or roof shape) and the vulnerability classes.

In this study, we applied a popular method, called association rule learning (ARL; Agrawal et al. 1993), relevant to seismic vulnerability application (Riedel et al. 2014, 2015). Applied to the CBD, conditional probabilities between basic structural

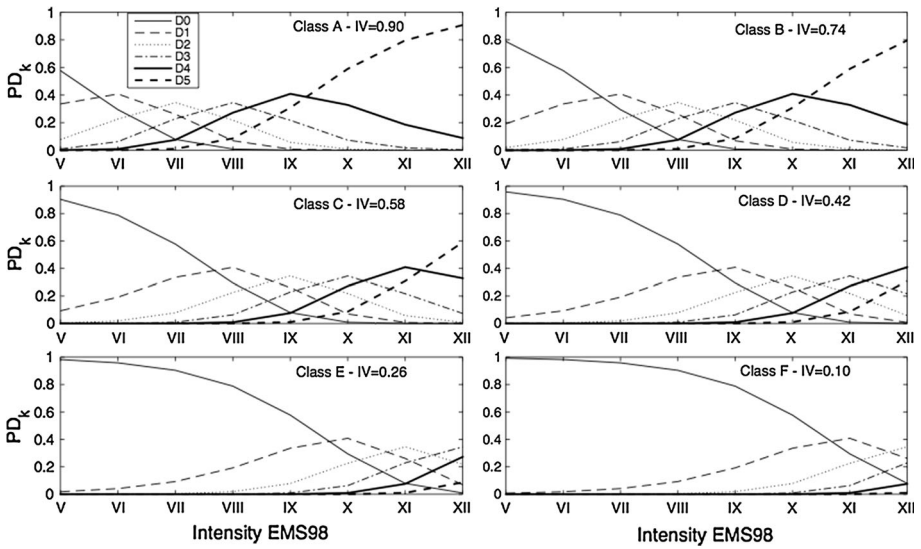


Fig. 4 Probability of exceeding damage $P(D_k)$ for each class of vulnerability computed for macro-seismic intensities V–XII (according to Eq. 3 and Lagomarsino and Giovinazzi 2006)

information (attribute X) and EMS-98 vulnerability classes (target $Y = A, B, C, D, E$) are derived to give the Constantine vulnerability proxy (CVP). Association rules also take the form $X \rightarrow Y_i$, where X (consequent) and Y_i (antecedent) are two sets of independent items. Each relationship between X and Y_i can be represented in binary format [0,1]: Knowing the building attributes X , the probability of belonging to class Y_i is expressed by

$$P(Y_i|X) = \frac{P(Y_i \cap X)}{P(X)} \tag{4}$$

or in practice, $P(Y_i|X)$ can be calculated as:

$$P(Y_i|X) = \frac{N_{XY}}{N_X} \tag{5}$$

where N_x is the total number of buildings with attribute X and N_{xy} the number of buildings with attribute X and belonging to class Y_i . One limitation of the ARL method is that by searching massive numbers of possible associations, there is a significant risk that the results will include inconsistencies, due to false associations. We used two phases applied to the CBD in order to test the efficiency of the CVP.

3.2.1 First phase: learning

Once the databank was ready, a learning phase was applied to a subset of data. The size of the learning subset was chosen according to the results obtained by Riedel et al. (2015). They found that the quality of an estimate reaches an asymptote beyond a size of learning subset representing 30% of the total data, and we assumed for this study the same size of subset. We therefore selected 2500 sets of data randomly, each representing 30% of the whole databank. Classification accuracy is sensitive to the dataset; so many combinations

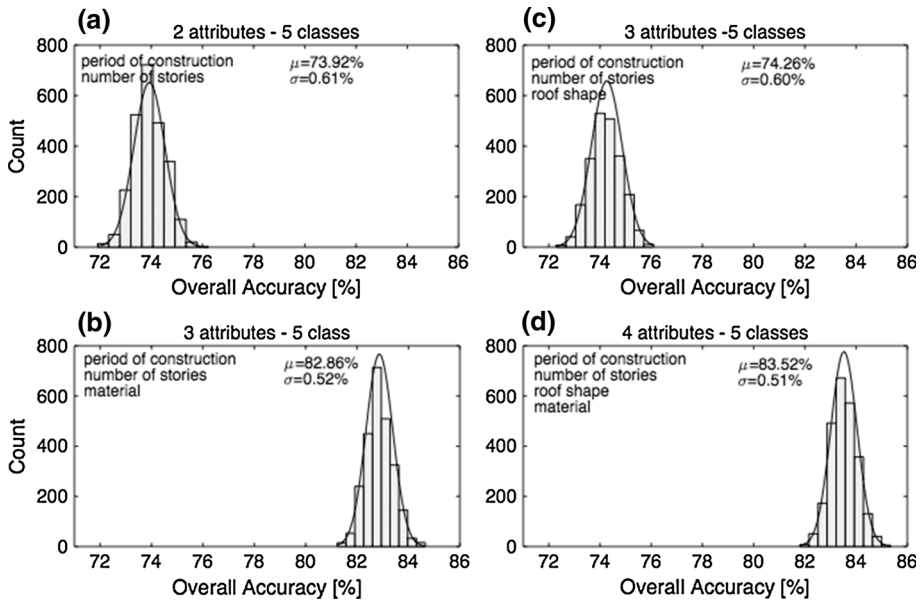


Fig. 5 Accuracy of the vulnerability classification considering 2500 random subsets of 30% of the buildings in the Constantine Building Databank for several attribute combinations: **a** construction period and number of stories; **b** construction period, number of stories and material; **c** construction period, number of stories and roof shape; **d** construction period, number of stories, material, and roof shape

were then tested considering one or several of the basic attributes (i.e., period of construction, number of stories, material and roof). Classification accuracy is shown in Fig. 5 as the percentage of correctly classified classes of vulnerability for a given combination of attributes.

By applying ARL, we observed that the classification (i.e., assessment of vulnerability classes) is quite relevant even when only basic information is considered. Firstly, for all cases, variability of the accuracy distribution is less than 1%, reflecting the independence of subset selection for the classification ($\sigma \leq 0.61\%$). Secondly, mean accuracy is over than 73% for two single attributes (period of construction and number of stories), reaching about 83% for combinations including material. This attribute is considered to be a key parameter, having significant weight in the vulnerability assessment. However, as reported by Riedel et al. (2015), period of construction and material are two dependent attributes (e.g., 98% of buildings built before 1920 were unreinforced masonry constructions, and after 1962 all were RC), inferring that the benefit in terms of accuracy of considering material is rather limited. This is certainly the most difficult attribute to assess accurately and a balance between cost and accuracy of the inventory by visual screening and quality of the classification must be evaluated before starting a survey. We also observed that by adding roof shape, classification is slightly improved, suggesting correlation of this attribute with the others.

Table 4 Conditional probability for each EMS-98 vulnerability class according to building attribute (period of construction, number of stories) obtained using the ARL method

Attributes	P(A)	P(B)	P(C)	P(D)	P(E)
] < 1837]—LR	0.827	0.173	0	0	0
] < 1837]—MR	0.833	0.167	0	0	0
] < 1837]—HR	/	/	/	/	/
]1837–1920]—LR	0.158	0.710	0.053	0	0.079
]1837–1920]—MR	0.238	0.720	0.042	0	0
]1837–1920]—HR	0.200	0.400	0.400	0	0
]1920–1962]—LR	0.098	0.727	0.168	0	0.007
]1920–1962]—MR	0.103	0.603	0.294	0	0
]1920–1962]—HR	0.158	0.052	0.790	0	0
]1962–1981]—LR	0	0.181	0.455	0	0.364
]1962–1981]—MR	0	0	1.000	0	0
]1962–1981]—HR	0	0	1.000	0	0
]1981–2003]—LR	0	0	0	1.000	0
]1981–2003]—MR	0	0	0.250	0.667	0.083
]1981–2003]—HR	0	0	0	1.000	0
] > 2003]—LR	0	0	0	0	1.000
] > 2003]—MR	0	0	0.050	0	0.950
] > 2003]—HR	0	0	0	0	1.000

/ mean no data

3.2.2 Second phase: validation on the rest of the Constantine Building Databank

After completion of the learning phase, the vulnerability proxy (CVP) was defined for all combinations and vulnerability classes. Table 4 shows the conditional values (i.e., CVP) of classification in the EMS98 vulnerability classes, knowing the two most basic building attributes (i.e., period of construction and number of stories). For example, a randomly selected building in Constantine known to have been built before 1837 and with less than 2 floors has a probability of 82.7% of being in Class A and 17.3% of being in Class B.

This proxy was then applied to the rest of the CBD, i.e., 70% of the databank, considering several attribute combinations and vulnerability classes. The buildings were then grouped into subsets or, in our case, into geographical units. The vulnerability within each unit was then expressed as the probability of being in class *j*, as follows:

$$P_j(Y) = \sum_1^N \frac{N_{ji}P(Y|X_i)}{N} \tag{6}$$

with $P_j(Y)$ the probability of one building being in class $Y_i = \{A, B, C, D, E\}$, N_{ji} being the number of buildings with attributes X_i in class Y_j , $P(Y|X_i)$ the proxy value in Table 4 and N the number of buildings. Table 5 shows an example of a confusion matrix that compares the predicted vulnerability with the ground truth for three attributes (period of construction, number of stories, roof shape) and five classes. The values on the diagonal are the buildings that were assigned correctly.

In this example, overall accuracy of construction assignment is 74.24%. Accuracy was lower for classes A and B: 261 class A buildings were correctly classified but 191 and 6

Table 5 Example of a confusion matrix obtained with the ARL method to classify the buildings in Constantine into EMS98 seismic vulnerability classes based on three attributes

EMS-98 class	Vulnerability (ARL classification)					Accuracy (%)
	A	B	C	D	E	
<i>Vulnerability (ground truth)</i>						
A	261	191	6	0	0	56.99
B	49	706	10	1	1	92.05
C	3	130	121	1	2	47.08
D	0	0	1	22	0	95.65
E	0	7	2	2	60	84.51
Accuracy	83.39%	68.28%	86.43%	84.62%	95.24%	74.24

Bold values correspond to the perfect assessment of vulnerability

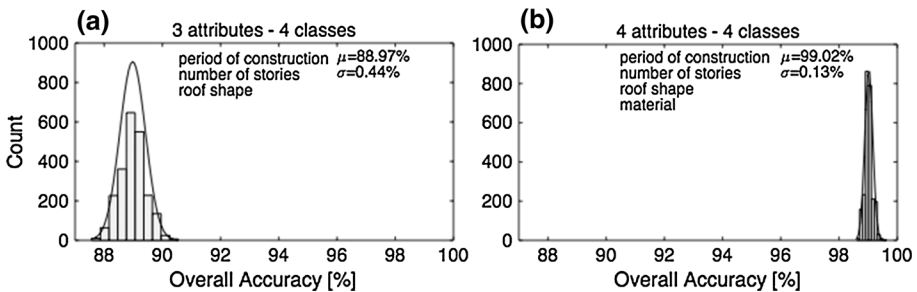


Fig. 6 Accuracy of the vulnerability classification considering 2500 random subsets of 30% of the buildings in the Constantine Building Databank, merging classes A and B, and for two attribute combinations: **a** construction period, number of stories and roof shape; **b** construction period, number of stories, material, and roof shape

buildings were incorrectly classified in B and C; 706 class B buildings were correctly classified but 49 and 10 were misclassified in A and C, respectively. As observed by Riedel et al. (2014), distinguishing between classes A and B is difficult because of the equivalent vulnerability associated with the different types of buildings, according to EMS98. Most of the misclassified class A buildings are actually in B, and we can improve classification accuracy by merging these two classes. For classes C, D and E, the accuracy of the classification is better, with 86, 85 and 95% of well-classified buildings. Figure 6 shows the overall accuracy of the classification considering four classes, i.e., after merging A and B. Considering 3 attributes (period of construction, number of stories, roof shape), accuracy increases to 89 and to 99% if the material attribute is also included, with very slight variability (0.13%).

In the rest of the paper, we used the CVP proxy given in Table 4 requiring only two attributes. The purpose is to extend the proxy to other Algerian cities, based on only these two parameters. The need for only two attributes eliminates one of the main difficulties related to any vulnerability study, while remaining relevant at the urban scale. Application of the proxy to other Algerian cities means assuming that the characteristics of the Constantine urbanization are similar in all cities throughout the region: This can be a weak

Table 6 Damage probability matrix for vulnerability class A interpreted according to EMS98 (after Riedel et al. 2015)

	Damage grade					
	D0	D1	D2	D3	D4	D5
<i>Intensity EMS98</i>						
IV	1.00	0.00	0.00	0.00	0.00	0.00
V	0.95	0.05	0.00	0.00	0.00	0.00
VI	0.60	0.35	0.05	0.00	0.00	0.00
VII	0.05	0.20	0.35	0.35	0.05	0.00
VIII	0.00	0.05	0.20	0.35	0.35	0.05
IX	0.00	0.00	0.05	0.25	0.35	0.35
X	0.00	0.00	0.00	0.00	0.20	0.80
XI	0.00	0.00	0.00	0.00	0.00	1.00
XII	0.00	0.00	0.00	0.00	0.00	1.00

assumption at the first order as shown by Riedel et al. (2015). Finally, we compared the results of the vulnerability assessment by ARL with the mean values of vulnerability given by Risk-UE. Having attributed the vulnerability classes, damage was computed following two strategies.

The first strategy, named ARL0 herein, is based on the EMS98 damage scale. For a given intensity, the number of buildings expected to suffer damage is defined by the terms “Few,” “Many” and “Most,” translated into numerical values 5, 35 and 80%, respectively (Lagomarsino and Giovinazzi 2006; Bernardini et al. 2010) and finally represented in a continuous manner by Riedel et al. (2015) to give the damage probability matrix given in Table 6 for vulnerability class A.

The damage probability for a given intensity $P_{EMS98}(D_k)$ is then computed by the equation:

$$P_{EMS98}(D_k) = \frac{1}{N} \sum_{i=A}^{i=E} N_i P(D_k|i, I_{EMS98}) \tag{7}$$

where N is the total number of buildings, N_i the number of buildings with vulnerability class i ($i = A, B, C, D, E$) and $P(D_k|i, I_{EMS98})$ the probability of damage grade D_k for a given vulnerability class i and intensity I_{EMS98} provided in Table 6.

The second strategy, called ARL1, uses the Risk-UE damage probability model (Eq. 3), considering the relationship between the EMS98 vulnerability class and the Risk-UE vulnerability index (Lagomarsino and Giovinazzi 2006; Bernardini et al. 2010), as shown in Fig. 4.

4 Results

4.1 The vulnerability map of Constantine

Figure 7 shows vulnerability in zones 1, 2 and 3 computed by Risk-UE and based on the EMS98 classification. Almost 80% of the buildings have a Risk-UE vulnerability index

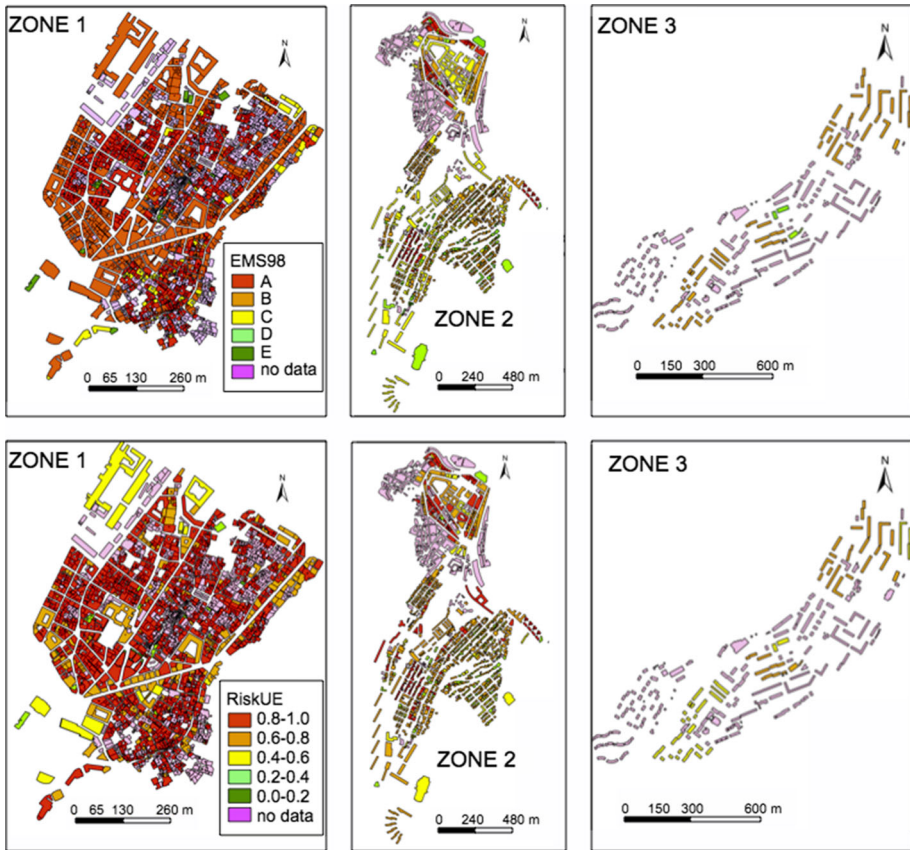


Fig. 7 Vulnerability distribution in zones 1, 2 and 3 of Constantine, represented by the EMS98 classes assigned using the ARL method (*upper row*) and using the Risk-UE indexes (*lower row*)

over than 0.70, which is equivalent to vulnerability classes A and B. In comparison, 78% of the buildings are classified as A and B according to the ARL method, which confirms the efficiency of the datamining-based method to assess vulnerability at the urban scale with basic building attributes compared to a more sophisticated method (Risk-UE). We observe that zone 1, corresponding to the historic center, is the most vulnerable, with classes A and B. This area was built before 1837 and partially between 1837 and 1920, with 94% of unreinforced masonry constructions. The rest were built during the French period, where most of buildings were designed without earthquake engineering. In zone 2, built between 1920 and 1962, the ARL proxy classified the majority of buildings in the northern part of the zone in A and B, indicating a mix of all classes for the southern area. This is the most heterogeneous area, which contains buildings of all construction periods. The modern part of the city corresponds to zone 3, urbanized mainly between 1962 and 1981, composed only of RC buildings (frame and shear walls) and characterized by the least vulnerable classes (C and D). Based on the correlation between the Risk-UE indexes and the EMS98 classes, the distributions of the most vulnerable buildings are roughly similar, with a slight

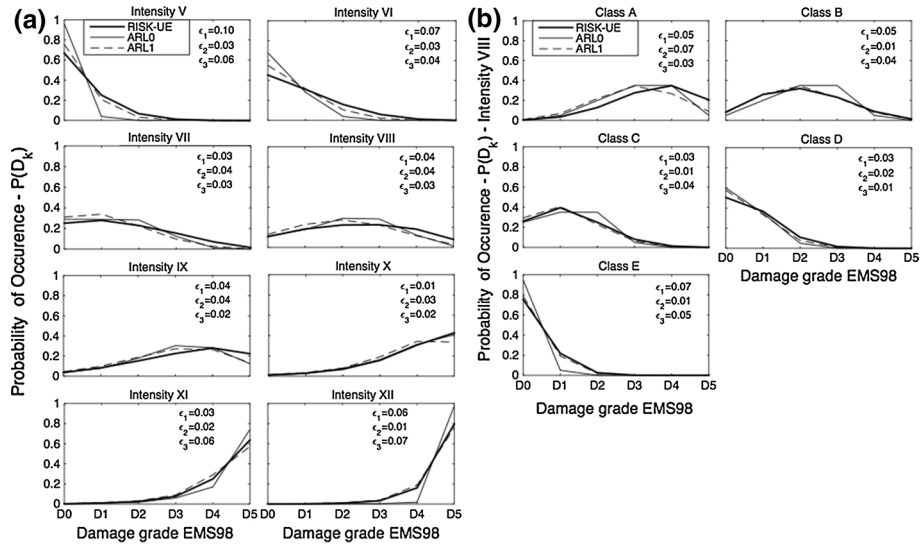


Fig. 8 Probability of exceeding damage $P(D_k)$ **a** for intensities between V and XII computed with the ARL0, ARL1 and Risk-UE methods and **b** for intensity VIII and vulnerability classes A–E. ϵ_1 is the absolute error between Risk-UE and ARL0, ϵ_2 between ARL1 and Risk-UE and ϵ_3 between ARL0 and ARL1

difference in geographic distribution. A building-by-building comparison could be conducted, but in order to be consistent with the statistical approach required for vulnerability assessment at global scale, the comparison will be based on the probability to exceed damage per geographical unit.

4.2 Damage assessment

The probability $P(D_k)$ of exceeding damage level D_k was computed according to three different approaches: the Risk-UE model (Eq. 3), the ARL0 and ARL1 methods, considering a spatially uniform seismic. For this comparison, only intensity is considered without accounting for eventually additional effects such as site effects, soil nonlinearity or triggered effects (e.g., landslides) that might modify the seismic hazard. In order to check the relevancy of the ARL methods in terms of damage prediction, we computed the total absolute error ϵ of predicted damage $P(D_k)$ considering all damage grades k and different macro-seismic intensity scenarios (Fig. 8): ϵ_1 between Risk-UE and ARL0, ϵ_2 between ARL1 and Risk-UE and ϵ_3 between ARL0 and ARL1. Overall, we found $\epsilon_2 < \epsilon_1 < \epsilon_3$. The differences between Risk-UE and ARL1 (ϵ_2) are mainly due to the seismic vulnerability assessment methods; the differences between ARL0 and ARL1 (ϵ_3) are due to the model for computing damage with the same vulnerability; and the differences between Risk-UE and ARL0 (ϵ_1) are a combination of the two.

For all intensities (Fig. 8a), the absolute error is very small, with the largest values for the two extreme intensities equal to 0.10, 0.07, 0.06 and 0.06 for ϵ_1 , 0.06, 0.04, 0.06 and 0.07 for ϵ_3 for intensities V, VI, XI and XII, respectively. The smallest error corresponds to ϵ_2 , i.e., the error for the damage model (Risk-UE) but using two different models for vulnerability assessment. This confirms that for damage prediction, assessing seismic

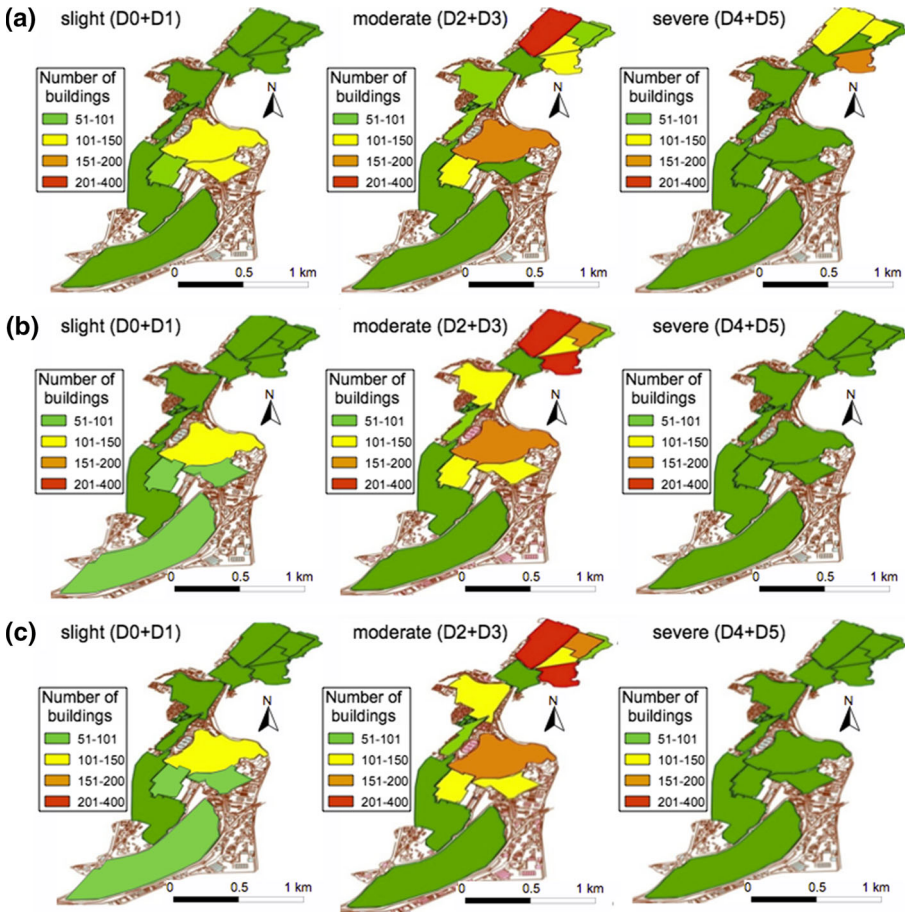


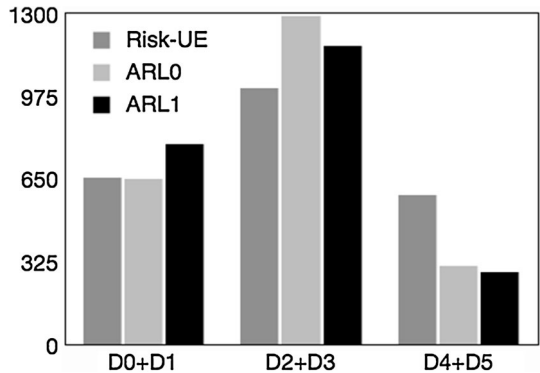
Fig. 9 Spatial distribution of damage in Constantine computed for the intensity VIII scenario. Damage levels are grouped into slight ($D_0 + D_1$), moderate ($D_2 + D_3$) and severe ($D_4 + D_5$) and given as the number of buildings: **a** ARL0 method; **b** ARL1 method; **c** Risk-UE method

vulnerability using the ARL method provides the same magnitude of damage as Risk-UE, with differences of less than 0.04. For the highest intensities (XI and XII), we obtained the same probability of exceedance with both ARL0 and ARL1: For these intensities, the generalization of damage to the most vulnerable buildings smooths the error related to damage prediction.

For a given intensity VIII (Fig. 8b), the largest errors were observed for vulnerability classes A and E, with values equal to 0.05 and 0.07 for ϵ_1 and ϵ_3 . ϵ_2 often has the lowest values (classes B, C and E) and remains very low except for class A. The probabilities $P(D_k)$ are therefore comparable, regardless of the methods used for damage and vulnerability assessment. This confirms that with only two attributes, damage predictions are reliable even if vulnerability may be slightly variable. This remark is important because at the scale of the city, it means that an individual building inventory is not necessary to collect data on all the attributes and modifiers required to assess the Risk-UE index. An alternative is to use

Table 7 Comparison of the damage distribution (number of buildings and percentage) obtained by ARL and Risk-UE in Constantine for intensity VIII

	D0 + D1		D2 + D3		D4 + D5	
Risk-UE	655	29.1%	1008	44.8%	589	26.2%
ARL0	654	29.0%	1288	57.2%	310	13.8%
ARL1	791	35%	1172	52.0%	289	13.0%

Fig. 10 Comparison of the number of damaged buildings for intensity VIII computed by Risk-UE and ARL methods

existing data, for example, from preexisting national databases or collected by remote sensing for the roof shape and the number of stories, or a combination of both.

4.3 Comparing the seismic damage scenario for Constantine

Figure 9 presents the damage distribution obtained for a given seismic scenario (intensity VIII) considering the same intensity throughout Constantine. This scenario corresponds to the last major earthquake that hit the region in 1985 ($I = VIII$). The three zones are divided into subzones, defined as being homogenous in terms of urbanization (construction period and typology). We observed similar results for the three approaches.

The scenario results for zone 1 (i.e., the oldest part of the city) indicate moderate to severe damage according to the Risk-UE method and moderate damage for both ARL0 and ARL1 methods. This is mainly due to the poor quality of buildings in this zone, with 94% of buildings classified as A or B, zone 1 being mainly composed of unreinforced masonry buildings (95% of the building stock). This area corresponds to a densely urbanized zone, with residential and commercial buildings. Zones 2 and 3 may suffer slight to moderate damage, because of the presence of a majority of frame and shear-wall RC buildings (urbanized between 1920 and 1980).

The damage distribution for Risk-UE and ARL methods is given in Table 7 and shown in Fig. 10. For an earthquake comparable to the 1985 earthquake ($I = VIII$), the damage level computed by Risk-UE shows that nearly 29% of the buildings of the studied area would be undamaged or only slightly damaged (D0 + D1), while about 45% of buildings would suffer moderate damage (D2 + D3), and more than 25% of buildings would suffer

severe damage (D4 + D5). Using ARL, similar results are obtained for slight damage (29%), and differences are observed for moderate (57%) and severe damage (14%), resulting from the difficulties encountered sometimes in distinguishing classes A and B. Nevertheless, in terms of damage prediction for seismic risk management and anticipation, both results are very similar and allow representation of the seismic risk required to implement a seismic risk management policy.

5 Conclusions

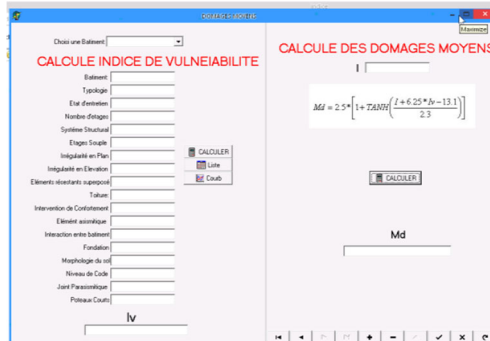
One of the largest challenges in seismic vulnerability analysis at the urban scale is to compensate for the lack or poor quality of information concerning construction characteristics, and this is certainly the most costly step of any seismic risk analysis. To overcome this problem, a recent approach was tested for the city of Constantine, based on the ARL datamining method. In this manuscript, we have shown the possibility of using simplified analysis methods, using single building type attributes to represent and analyze the seismic risk at the urban scale. This will enable more detailed studies of existing buildings and the assessment of future seismic measures.

One of the most significant characteristics of this method is that it extracts “hidden” relationships between elementary attributes of buildings and seismic vulnerability. A vulnerability proxy is then derived to attribute the vulnerability class for all combinations of building attributes. The proxy was derived during a learning phase and then applied to the rest of the databank of Constantine’s buildings. We observed robust and accurate assessment of vulnerability, regardless of the building subset used for the learning phase and compared to the Risk-UE vulnerability assessed in Constantine considered as the ground truth. The accuracy of the ARL method was evaluated in comparison with the Risk-UE method, which requires a lot of information on building characteristics. Comparison of results showed that the two approaches provide similar results. This suggests that the ARL methodology was successfully applied to the Constantine data. We observed that considering the same damage model, vulnerability assessment by ARL provides the same damage estimate as Risk-UE, even if only two attributes are used. We confirmed that vulnerability assessment using the datamining approach provides a relevant estimation of seismic damage at a cost far lower than that of conventional methods, such as Risk-UE. In case of structural modification or retrofitting, ARL-based classification might be updated in the same manner as the Risk-UE vulnerability, and the date and the nature of modification could be considered as an additional attribute for the classification. Finally, the ARL method was able to give an overall assessment of seismic risk in an urban area. Assuming similar urbanization features through Algeria, the ARL-based vulnerability proxy derived for Constantine could be applied to other cities to enable seismic vulnerability and seismic risk to be assessed at the scale of the country, using national census data or remote sensing data.

Acknowledgements The MAIF Foundation supported this work. Philippe Guéguen has been supported by a grant from Labex OSUG@2020 (Investissements d’avenir—ANR10 LABX56).

Appendix 1: Building inventory form used in Constantine and screenshot (in French) of the automatic datasheet used to compute vulnerability index and mean damage using Risk-UE method

ID:	Address of building:	Date of inspection:
General information <u>Building inspection:</u> <input type="checkbox"/> Outside <input type="checkbox"/> Inside <input type="checkbox"/> Outside - Inside <u>Year of built :</u> <input type="checkbox"/> <1837 <input type="checkbox"/> 1837-1920 <input type="checkbox"/> 1921-1962 <input type="checkbox"/> 1963-1981 <input type="checkbox"/> 1982-2003 <input type="checkbox"/> > 2003 <u>Year of seismic codes:</u> <input type="checkbox"/> <1981 :Low <input type="checkbox"/> 1981-2003 Moderate <input type="checkbox"/> >2003 High <u>Number of stories :</u> <input type="checkbox"/> 1-2 <input type="checkbox"/> 3-5 <input type="checkbox"/> ≥ 6 <u>Material:</u> <input type="checkbox"/> Masonry <input type="checkbox"/> Reinforced Concrete <input type="checkbox"/> Steel <input type="checkbox"/> Wood <u>Type of slabs :</u> <input type="checkbox"/> RC slabs <input type="checkbox"/> Wood slabs <input type="checkbox"/> steel and masonry slabs <u>Irregular configuration in plan:</u> <input type="checkbox"/> yes <input type="checkbox"/> No <u>Vertical irregularities or discontinuities:</u> <input type="checkbox"/> yes <input type="checkbox"/> No <u>Aggregate effect: building position:</u> <input type="checkbox"/> Middle <input type="checkbox"/> Corner <input type="checkbox"/> Header <u>Aggregate building: elevation:</u> <input type="checkbox"/> Staggered floors <input type="checkbox"/> different height <u>Number of occupants:</u>		LEGAL STATUS: PUBLIC: <input type="checkbox"/> <input type="checkbox"/> Administrative <input type="checkbox"/> commercial <input type="checkbox"/> equipment PRIVATE: <input type="checkbox"/> Type : <input type="checkbox"/> Collective <input type="checkbox"/> Individual
General conditions of the building <u>State of preservation :</u> <input type="checkbox"/> Good <input type="checkbox"/> Bad <input type="checkbox"/> Very bad <u>Retrofitting interventions :</u> <input type="checkbox"/> yes <input type="checkbox"/> No <input type="checkbox"/> year of interventions : <u>Soil morphology:</u> <input type="checkbox"/> Slope <input type="checkbox"/> Cliff		
Structural conditions <u>Structural type:</u> <input type="checkbox"/> Reinf Masonry <input type="checkbox"/> Unrein Masonr <input type="checkbox"/> RC Moment Frame <input type="checkbox"/> RC Shear Wal <input type="checkbox"/> RC Dual system <input type="checkbox"/> Precast RC wall <u>Soft story :</u> <input type="checkbox"/> yes <input type="checkbox"/> No <input type="checkbox"/> Demolition <input type="checkbox"/> transparency <u>Seismic joint :</u> <input type="checkbox"/> sufficient <input type="checkbox"/> insufficient <u>Foundations types :</u> <input type="checkbox"/> isolated <input type="checkbox"/> strip footings <input type="checkbox"/> strip footings + beams foundations at different levels: <input type="checkbox"/> yes <input type="checkbox"/> No		
non-structural elements: <u>Aseismic Devices :</u> <input type="checkbox"/> Barbican <input type="checkbox"/> Foil <input type="checkbox"/> arches <input type="checkbox"/> Buttresses <u>Bow windows :</u> <input type="checkbox"/> yes <input type="checkbox"/> No		



Appendix 2: On site pictures of inspected buildings in Constantine



References

- Agrawal R, Imielinski T, Swami A (1993) Mining association rules between sets of items in large databases. In: Proceedings of the 1993 ACM SIGMOD international conference on Management of data, SIGMOD '93. doi:[10.1145/170035.17007](https://doi.org/10.1145/170035.17007)
- Aoudia A, Meghraoui M (1995) Seismotectonics in the Tell Atlas of Algeria: the Cavaignac (Abou El Hassan) earthquake of 25.08. 1922 ($M_s = 5.9$). *Tectonophysics* 248(3):263–276
- Baba Hamed FZ, Rahal DD, Rahal F (2013) Seismic risk assessment of Algerian buildings in urban area. *J Civ Eng Manag* 19(3):348–363
- Barbat AH, Carreño ML, Pujades LG, Lantada N, Cardona OD, Marulanda MC (2010) Seismic vulnerability and risk evaluation methods for urban areas. A review with application to a pilot area. *Struct Infrastruct Eng* 6:17–38. doi:[10.1080/15732470802663763](https://doi.org/10.1080/15732470802663763)
- Bard P-Y, Duval A-M, Bertrand E, Vassiliadès J-F, Vidal S, Thibault C, Guyet B, Mèneroud J-P, Guéguen P, Foin P, Dunand F, Bonnefoy-Claudet S, Vettor G (2005) Le risque Sismique à Nice: apport méthodologique, résultats et perspectives opérationnelles. Rapport final GEMGEP
- Benedetti D, Petriani V (1984) Sulla vulnerabilità di edifici in muratura: proposta di un metodo di valutazione. *L'industria delle Costruzioni* 149:66–74 (in Italian)
- Benson C, Twigg J (2004) Measuring mitigation: methodologies for assessing natural hazard risks and the net benefits of mitigation—a scoping study. In: International Federation of Red Cross and Red Crescent Societies/the ProVention Consortium
- Bernardini A, Lagomarsino S, Mannella A, Martinelli A, Milano L, Parodi S (2010) Forecasting seismic damage scenarios of residential buildings from rough inventories: a case-study in the Abruzzo Region (Italy). *Proc Inst Mech Eng Part O J Risk and Reliab* 224(4):279–296
- Boukri M, Farsi MN, Mebarki A, Belazougui M, Amellal O, Mezagzigh B, Guessoum N, Bourenane H, Benhamiuche A (2014) Seismic risk and damage prediction: case of the buildings in Constantine city (Algeria). *Bull Earthq Eng* 12:2683–2704. doi:[10.1007/s10518-014-9594-0](https://doi.org/10.1007/s10518-014-9594-0)

- Bounif A, Haessler H, Meghraoui M (1987) The Constantine (northeast Algeria) earthquake of October 27, 1985: surface ruptures and aftershock study. *Earth Planet Sci Lett* 85(4):451–460
- Bufo E, De Galdeano CS, Udías A (1995) Seismotectonics of the Ibero-Maghrebian region. *Tectonophysics* 248(3):247–261
- Chatelain JL, Tucker B, Guillier B, Kaneko F, Yepes H, Fernandez J, Yamada T (1999) Earthquake risk management pilot project in Quito, Ecuador. *GeoJournal* 49(2):185–196
- Erdik M, Aydinoglu N, Fahjan Y, Sesetyan K, Demircioglu M, Siyahi B, Yuzugullu O (2003) Earthquake risk assessment for Istanbul metropolitan area. *Earthq Eng Eng Vib* 2(1):1–23
- Faccioli E, Pessina V, Calvi GM, Borzi B (1999) A study on damage scenarios for residential buildings in Catania city. *J Seismol* 3(3):327–343
- Geiß C, Taubenböck H, Tyagunov S, Tisch A, Post J, Lakes T (2014) Assessment of seismic building vulnerability from space. *Earthq Spectra* 30(4):1553–1583
- GNDT (1993) *Rischio Sismico di edifici Pubblici-Parte I Aspetti Metodologici*. CNR – Gruppo Nazionale per la Difesa dai Terremoti, Roma, Italy (in Italian)
- Grünthal G, Levret A (2001) L'échelle macrosismique européenne, European macroseismic scale 1998(EMS-98), Conseil de l'Europe, Cahiers du Centre Européen de Géodynamique et de Séismologie, vol 19
- Guéguen P (ed) (2013) *Seismic vulnerability of structures Civil Engineering and geomechanics series*. John Wiley and son, Hoboken, 368 pp
- Guéguen P, Michel C, LeCorre L (2007) A simplified approach for vulnerability assessment in moderate-to-low seismic hazard regions: application to Grenoble (France). *Bull Earthq Eng* 4(3):467–490
- Hamdache M, Peláez JA, Talbi A, Mobarki M, Casado CL (2012) Ground-motion hazard values for Northern Algeria. *Pure Appl Geophys* 169(4):711–723
- HAZUS (1997) *Earthquake loss estimation methodology*, Hazus technical manuals. National Institute of Building Science, Federal Emergency Management Agency (FEMA), Washington
- Kherroubi A, Déverchère J, Yelles A, De Lépinay BM, Domzig A, Cattaneo A, Graindorge D (2009) Recent and active deformation pattern off the easternmost Algerian margin, Western Mediterranean Sea: new evidence for contractional tectonic reactivation. *Mar Geol* 261(1):17–32
- KVERMP (1998) The Kathmandu Valley earthquake management action plan. <http://geohaz.org/downloads/publications/KathmanduValleyEQRiskMgtActionPlan.pdf>
- Lagomarsino S, Giovinazzi S (2006) Macroscopic and mechanical models for the vulnerability and damage assessment of current buildings. *Bull Earthq Eng* 4(4):415–443
- Lestuzzi P, Podestà S, Luchini C, Garofano A, Katzantzidou-Firtinidou D, Bozzano C, Bischof P, Haffter A, Rouiller J-D (2016) Seismic vulnerability assessment at urban scale for two typical Swiss cities using Risk-UE methodology. *Nat Hazards*. doi:10.1007/s11069-016-2420-z
- McKenzie D (1972) Active tectonics of the Mediterranean region. *Geophys J Int* 30(2):109–185
- Meslem A, Yamazaki F, Maruyama Y, Benouar D, Kibboua A, Mehani Y (2012) The effects of building characteristics and site conditions on the damage distribution in Boumerdès after the 2003 Algeria earthquake. *Earthq Spectra* 28(1):185–216
- Mickus K, Jallouli C (1999) Crustal structure beneath the Tell and Atlas Mountains (Algeria and Tunisia) through the analysis of gravity data. *Tectonophysics* 314(4):373–385
- Milutinovic ZV, Trendafiloski GS (2003) Risk-UE an advanced approach to earthquake risk scenarios with applications to different European towns, Contract: EVK4-CT-2000-00014, WP4: Vulnerability of Current Buildings
- Mueller M, Segl K, Heiden U, Kaufmann H (2006) Potential of high-resolution satellite data in the context of vulnerability of buildings. *Nat Hazards* 38(1–2):247–258
- ONS (2008) General census of housing and population, National Statistics Office, Algiers
- Ousadou F, Dorbath L, Dorbath C, Bounif MA, Benhallou H (2013) The Constantine (Algeria) seismic sequence of 27 October 1985: a new rupture model from aftershock relocation, focal mechanisms, and stress tensors. *J Seismol* 17(2):207–222
- Peláez JA, Hamdache M, Casado CL (2006) Seismic hazard in terms of spectral accelerations and uniform hazard spectra in northern Algeria. *Pure Appl Geophys* 163(1):119–135
- Riedel I, Gueguen P, Dunand F, Cottaz S (2014) Macroscale vulnerability assessment of cities using association rule learning. *Seismol Res Lett* 85(2):295–305
- Riedel I, Guéguen P, Dalla Mura M, Pathier E, Leduc T, Chanussot J (2015) Seismic vulnerability assessment of urban environments in moderate-to-low seismic hazard regions using association rule learning and support vector machine methods. *Nat Hazards* 76(2):1111–1141. doi:10.1007/s11069-014-1538-0
- RPA03 (2003) Règles Parasismiques Algériennes/Algerian Earthquake Resistant Regulations RPA99/Version 2003, application since 2004, Ministère de l'Habitat et de l'Urbanisme

- RPA81 (1981) Règles Parasismiques Algériennes/Algerian Earthquake Resistant Regulations, Ministère de l'Habitat et de l'Urbanisme
- Smyth AW, Altay G, Deodatis G, Erdik M, Franco G, Gulkan P, Yuzugullu O (2004) Probabilistic benefit-cost analysis for earthquake damage mitigation: evaluating measures for apartment houses in Turkey. *Earthq Spectra* 20(1):171–203
- Spence R, Brun BL (2006) Preface. *Bull Earthq Eng* 4(4):319–321
- Tucker BE, Erdik MÖ, Hwang CN (eds) (2013) *Issues in urban earthquake risk*, vol 271. Springer Science & Business Media, Berlin
- Yelles-Chaouche A, Boudiaf A, Djellit H, Bracene R (2006) La tectonique active de la région nord-algérienne. *Comptes Rendus Géosci* 338(1):126–139